Hindawi Publishing Corporation
Journal of Nanomaterials
Volume 2014, Article ID 431956, 7 pages
http://dx.doi.org/10.1155/2014/431956

Research Article

Preparation of Cd-Loaded In_2O_3 Hollow Nanofibers by Electrospinning and Improvement of Formaldehyde Sensing Performance

Ruijin Hu, Jing Wang, Pengpeng Chen, Yuwen Hao, Chunli Zhang, and Xiaogan Li

School of Electronic Science and Technology, Dalian University of Technology, Dalian 116023, China

Correspondence should be addressed to Jing Wang; wangjing@dlut.edu.cn

Received 27 September 2013; Accepted 27 January 2014; Published 5 March 2014

Academic Editor: Artde Donald Kin-Tak Lam

Pure In_2O_3 and Cd-loaded In_2O_3 hollow and porous nanofibers with different Cd/In molar ratios (1/20, 1/10, 1/1) were synthesized by electrospinning method. X-ray diffraction (XRD), field emission scanning electron microscope (FE-SEM), and transmission electron microscopy (TEM) were used to characterize the nanofibers. The porous nanofibers were composed of small grains. The average grain sizes and the diameters of Cd-loaded In_2O_3 nanofibers increased with the increasing of Cd/In molar ratios. The formaldehyde sensing properties of the sensors based on pure In_2O_3 and Cd-loaded In_2O_3 nanofibers were investigated in formaldehyde concentration range of 0.5~100 ppm. Moreover, the selectivity of those sensors was studied by testing responses to methanol, toluene, ethanol, acetone, and ammonia. The result showed that Cd-loaded In_2O_3 nanofibers with Cd/In molar ratio of 1/10 possessed the highest response value and good selectivity at operating temperature 280°C. In addition, the formaldehyde sensing mechanism of the sensors based on Cd-loaded nanofibers was briefly analyzed.

1. Introduction

Formaldehyde is a hazardous indoor pollutant among volatile organic compounds (VOCs), and prolonged exposure to formaldehyde (HCHO) can cause serious health effects such as asthma, nasopharyngeal cancer, and multiple subjective health complaints [1]. Up to now, various materials prepared by different methods [2] were used to detect VOCs. Also the testing ways have been widely investigated [3–5]. Among these methods, gas sensor based on metal-oxide semiconductors (MOS) such as ZnO [6], SnO_2 [7], TiO_2 [8], and In_2O_3 [9] have been attracting special interest due to their good reproducibility, compact size, ease of use, and low cost.

In_2O_3, an important *n*-type semiconductor with a band gap of approximately 3.55–3.75 eV and good optical or electronic characters, has been widely used in solar cells, transparent conductors, and gas sensors. In recent years, gas sensors based on In_2O_3 with various morphologies have been investigated [10–12]. Among those morphologies, the controllable synthesis of one dimensional (1D) metal-oxide semiconductors nanofibers with high surface-to-volume ratio and effective electron transport have gained considerable attention in fabrication of miniature gas sensors [13–15]. In varieties of methods, electrospinning is a simple, effective, low-cost, and powerful approach to prepare 1D nanostructure nanomaterials including polymer, inorganic, and composite [16, 17].

In addition, noble metals [18–20], rare earth elements (REE) [21, 22], or metal oxide [23, 24] doping into MOS is a general method used to enhance the sensitivity, selectivity, and stability of gas sensors. And the metal additive acts as a catalyst to modify the surface reactions of MOS toward sensing gases [25]. Xu et al. prepared Au-loaded In_2O_3 nanofibers-based ethanol microgas sensor and found that the 0.2 wt% Au-loaded In_2O_3 based sensors possessed the characterization of high response, fast response/recovery, and low power consumption [26]. Wang et al. prepared Ag-doped In_2O_3 nanofibers by electrospinning and found that the response and recovery time of the sensors were about 5 and 10 s at low heating temperature of 115°C [21]. Xu et al. investigated room H_2S-sensing properties based on porous In_2O_3:REE (REE = Gd, Tb, Dy, Ho, Er, Tm, Yb) nanotubes

Table 1: Experimental parameters and characterized results.

Sample	$Cd(NO_3)_2{\cdot}4H_2O/In(NO_3)_3{\cdot}4.5H_2O$ (mg)	PVP (mg)	DMF/ethanol (mL)	Fiber diameter (nm)	Grain size (nm)
In_2O_3	0/764	917	5.6/7.0	156	26
$In_{20}Cd_1$	30.8/764	954	5.8/7.3	52	19
$In_{10}Cd_1$	61.6/764	1000	6.0/7.7	76	24
In_1Cd_1	308/383	830	5.0/6.4	88	42

and found that the response of the sensors based on In_2O_3 doped with Yb is around 7 times as much as pure In_2O_3 [27]. There are rare reports about gas sensors based on electrospun In_2O_3 nanofibers doped with common metal elements such as Cd.

In this report, In_2O_3 nanofibers doped with low-cost metal element Cd in different Cd/In molar ratios from 1/20 to 1/1 were synthesized by electrospinning method. Then HCHO gas sensor was fabricated by coating the obtained materials on the surface of the ceramic tube attached with Au belt-shaped electrodes. Then the sensing properties of sensors based on Cd-loaded In_2O_3 nanofibers with different Cd/In molar ratios were tested and discussed.

2. Experiment

2.1. Preparation of Pure In_2O_3 and Cd-Loaded Nanofibers. Poly(vinyl pyrrolidone) (PVP, $M_w = 1,300,000$) was purchased from Aldrich, USA. Indium nitrate ($In(NO_3)_3{\cdot}4.5H_2O$), cadmium nitrate ($Cd(NO_3)_2{\cdot}4H_2O$), N,N Dimethylformamide (DMF), and ethanol (EtOH) (99.0%) were obtained from Sinopharm Chemical Reagent Co., Ltd., China. All of the reagents used in the experiments were analytical grade and were utilized without further purification.

Cd-loaded In_2O_3 nanofibers were prepared by electrospinning method. In a typical procedure, 764 mg $In(NO_3)_3{\cdot}4.5H_2O$ power and 61.6 mg $Cd(NO_3)_2{\cdot}4H_2O$ were dissolved in 6.0 mL DMF and 7.7 mL ethanol under vigorous stirring for 2 h. Then 382 mg PVP was added to the above solution and stirred for 6 h to transparent precursor solution for electrospinning. The obtained solution was then loaded into syringe whose internal diameter of needle is 0.6 mm. The voltage applied to the needle was 18 kV and the distance between the needle and the collector was 15 cm. The as-electrospun $PVP/Cd(NO_3)_3{\cdot}4H_2O/In(NO_3)_3{\cdot}4.5H_2O$ composite nanofibers were annealed in tubular furnace at 500°C to obtain Cd-loaded In_2O_3 nanofibers with Cd/In molar ratio of 1/10. In the same way, pure In_2O_3 and Cd-loaded In_2O_3 with other Cd/In molar ratios were obtained as specific reagents proportion in Table 1.

2.2. Characterization of Cd-Loaded In_2O_3 Nanofibers. The structures of the nanofibers were characterized by an X-ray diffraction instrument (XRD: D/Max 2400, Rigaku, Japan) in 2θ region of 20~80° with Cu $K\alpha 1$ radiation. The morphology images of nanofibers were obtained by using field emission scanning electron microscope (FE-SEM: Hitachi S-4800, Japan) and by a transmission electron microscopy (TEM) using a Philips Fei Tecnai Sprit apparatus operated at 120 kV.

2.3. Fabrication and Measurement of Gas Sensors. As-prepared Cd-loaded In_2O_3 nanofibers with different Cd/In molar ratios of 1/20, 1/10, and 1/1 were marked as $In_{20}Cd_1$, $In_{10}Cd_1$, and In_1Cd_1, respectively, as shown in Table 1. The above four kinds of obtained nanofibers were diluted with deionized water in a mortar to form a paste, respectively. Then the paste was coated onto ceramic tube with a pair of gold electrodes to form a sensing film (150~200 μm). The ceramic tube was dried at 100°C in air for 2 h and subsequently annealedat 300°C for 5 h in tubular furnace. An Ni-Cr heating wire with 30 Ω as a heater was inserted through the tube to form an inside-heated gas sensor. The mechanism of test circuit and structure of the gas sensor were shown in Figure 1(a). Figure 1(b) gives the SEM picture of the $In_{10}Cd_1$ showing morphology and structure of nanofibers coated on the surface of the ceramic tube.

The gas-sensing properties of gas sensor based on Cd-loaded In_2O_3 nanofibers were measured using a static state gas-sensing test system [28]. The sensor was put into the test chamber for the sensing properties measurement. The environment temperature (18 ± 2°C) and relative humidity (~25% ± 5% RH) can be well controlled during the measurement. A fan was used to uniformly distribute the gas inside the chamber. The sensors were first heated by Ni-Cr heating wire for 10 min to stabilize the electrical properties of the sensor [29].

A given amount of target gas was injected into a test chamber (50 L in volume) by a syringe through a rubber plug. For a required concentration, the volume of the injected gas (V) can be calculated as:

$$V = \frac{50 \times C}{v\%}, \tag{1}$$

where C is the concentration of target gas (ppm: parts per million), and v% is volume fraction of bottled gas. The sensor was exposed to atmospheric air by opening the chamber after measurement. The gas response (S) was defined as a ratio of the sensor's electrical resistance in air (R_a) to that in target gas (R_g) as:

$$S = \frac{R_a}{R_g}, \tag{2}$$

where $R_a = R_L(10 - V_{\text{air}})/V_{\text{air}}$, $R_g = R_L(10 - V_{\text{gas}})/V_{\text{gas}}$, V_{air}, and V_{gas} are the voltages applied to the resistor R_L in air and in target gas, respectively. Response time t_{r1} and recovery time t_{r2} are defined as the time spent to achieve 90% of gas response change in adsorption and desorption process, respectively.

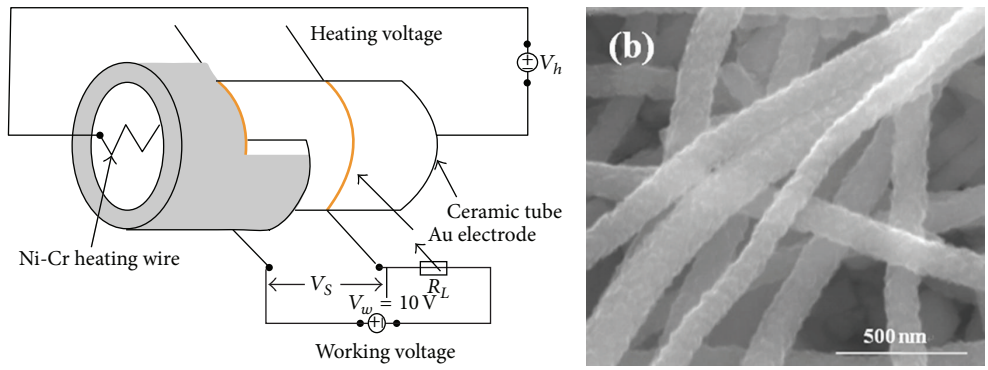

FIGURE 1: (a) The mechanism of test circuit and structure of the gas sensor and (b) SEM images of $In_{10}Cd_1$ nanofibers coated on the surface of the ceramic tube.

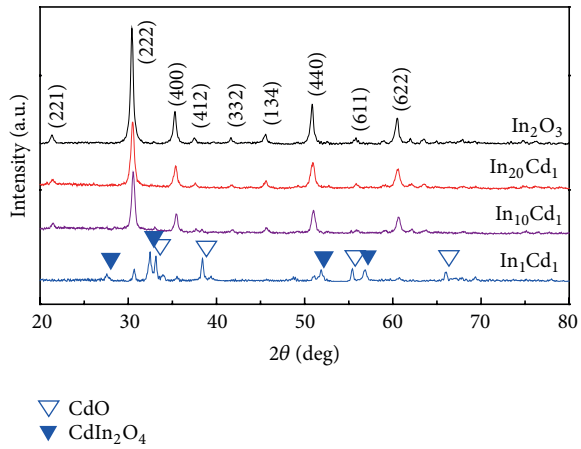

FIGURE 2: XRD patterns of pure In_2O_3 and Cd-loaded In_2O_3 nanofibers with different Cd/In molar ratios.

3. Results and Discussions

3.1. Morphologies and Structures of the as-Electrospun Cd-Loaded In_2O_3 Nanofibers. Figure 2 shows the XRD patterns of the pure In_2O_3 nanofibers and Cd-loaded In_2O_3 nanofibers with different Cd/In molar ratios. We can see that the In_2O_3 nanofibers calcined at 500°C possess strong and sharp diffraction peaks identifying a high degree of crystallization. All peaks in XRD patterns perfectly match the body-centered cubic structure of In_2O_3 (JCPDS: 65-3170). Meanwhile, there are no obvious Cd peaks in the pattern for $In_{20}Cd_1$ and $In_{10}Cd_1$ nanofibers, which may be due to the low concentration of Cd. And we can see that three kinds of diffraction peaks of In_2O_3, CdO, and $CdIn_2O_4$ appeared in curve of In_1Cd_1 nanofibers. According to the Scherrer equation, the average grain sizes of the nanofibers were around 26 nm, 19 nm, 24 nm, and 42 nm for pure In_2O_3, $In_{20}Cd_1$, $In_{10}Cd_1$, and In_1Cd_1, respectively.

The general morphologies of the as-electrospun pure In_2O_3 and Cd-loaded In_2O_3 nanofibers with different Cd/In molar ratios ($In_{20}Cd_1$, $In_{10}Cd_1$, and In_1Cd_1) were studied with SEM as shown in Figures 3(a)–3(d), respectively. It can be seen from Figure 3 that the average diameter of the after-annealed In_2O_3 nanofibers (~156 nm) is much bigger than that of Cd-loaded In_2O_3 nanofibers. And the average diameter of Cd-loaded In_2O_3 nanofibers increased with the increase of Cd/In molar ratios. Figures 3(b), 3(c), and 3(d) show obviously that the diameters of $In_{20}Cd_1$, $In_{10}Cd_1$, and In_1Cd_1 were 52 nm, 76 nm, and 88 nm, respectively. In addition, the inset in the top right corner of Figures 3(a)–3(d) shows the higher resolution TEM images of the corresponding nanofibers and we found that the as-prepared nanofibers with nanohierarchical structure were indeed composed of many interconnected grains. From the SEM and TEM graphs we can see that the average grain sizes of each nanofiber accorded with the results calculated by Scherrer equation basically. Further, the center of In_2O_3, $In_{20}Cd_1$, and $In_{10}Cd_1$ nanofibers in TEM images seemed much brighter than the black edge of nanofibers, which indicated that the hollow and porous structure formed in the three nanofibers.

3.2. Gas Sensing Properties of Cd-Loaded In_2O_3 Nanofibers. Figure 4 shows the responses of the pure In_2O_3 nanofibers and the Cd-loaded In_2O_3 nanofibers to 10 ppm of HCHO at different operating temperatures. It can be seen that the responses of these sensors depends on both the operating temperature and the concentration of Cd. In the range of the operating temperature studied, with the increasing of operating temperature, the response values firstly increased and then decreased for all the sensors. Each curve presents a maximum value at an optimum operating temperature. Besides, among all the sensors based on the above four kinds of nanofibers, the sensors based on $In_{10}Cd_1$ nanofibers exhibit the highest response when the operating temperature was 280°C.

Figure 5 shows the responses of the sensor based on pure In_2O_3, $In_{20}Cd_1$, $In_{10}Cd_1$, and In_1Cd_1 nanofibers to different concentrations of HCHO. The concentration range is 0.5–100 ppm. The inset in Figure 5 gives the responses versus low HCHO concentration in the range of 0.5~10 ppm. It can be seen that the responses of the sensors rapidly increased with increasing HCHO concentration from 0.5 ppm to 100 ppm. Compared with sensors based on other Cd-loaded In_2O_3

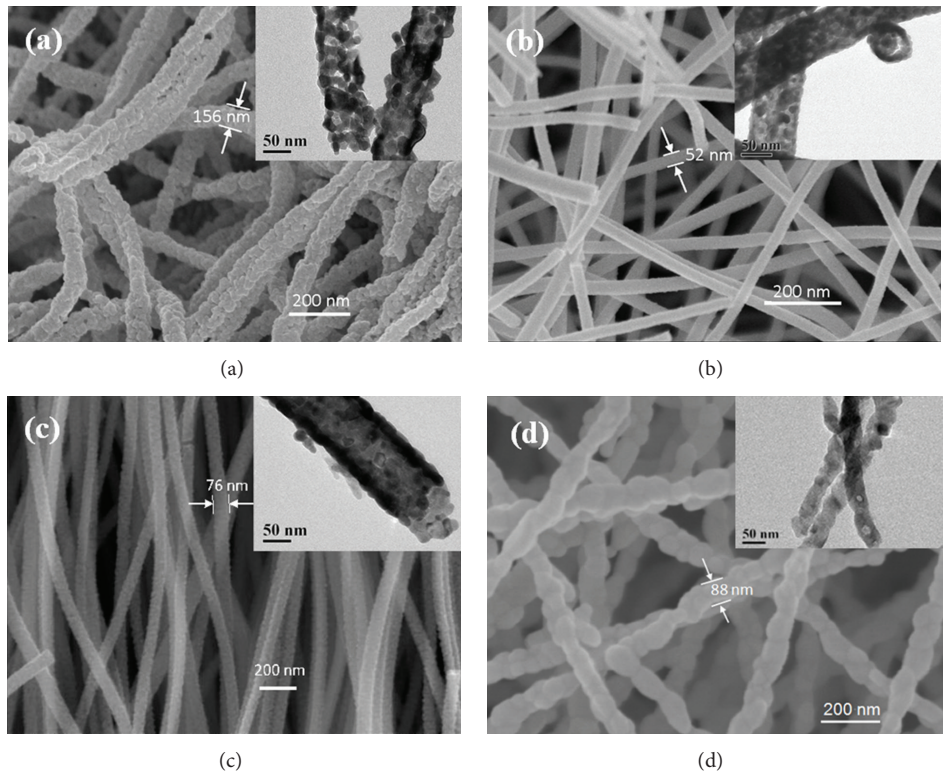

FIGURE 3: SEM images of (a) pure In_2O_3 nanofibers, (b) $In_{20}Cd_1$ nanofibers, (c) $In_{10}Cd_1$ nanofibers, and (d) In_1Cd_1 nanofibers; The inset in each graph is high magnification TEM image of each nanofiber.

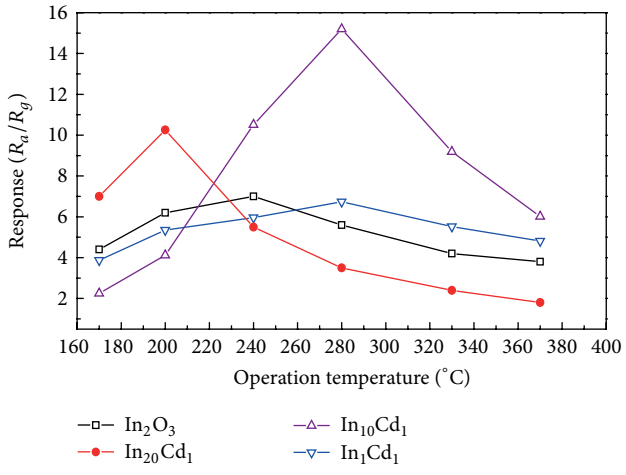

FIGURE 4: Responses of sensors based on pure In_2O_3 and Cd-loaded In_2O_3 nanofibers with different Cd/In molar ratios to 10 ppm HCHO as a function of operating temperature.

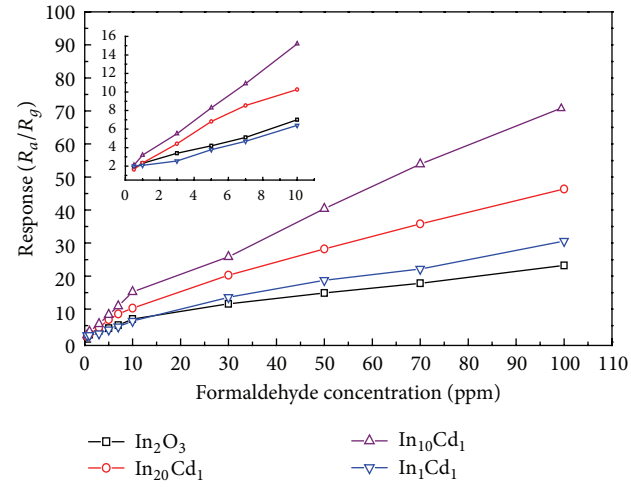

FIGURE 5: Response versus HCHO concentration for sensors based on pure In_2O_3 and Cd-loaded In_2O_3 nanofibers at each optimum operating temperature. The inset gives the responses versus low HCHO concentration.

nanofibers, the sensors based on $In_{10}Cd_1$ nanofibers show highest response, and there is a good linear correlation between the response of the sensors and the concentration of HCHO at high concentration range. So the specific and more HCHO-sensing properties of gas sensors based on $In_{10}Cd_1$ nanofibers will be discussed below.

Figure 6 shows the response and recovery transient properties of the gas sensor based on $In_{10}Cd_1$ nanofibers to formaldehyde in concentration range of 0.5~100 ppm at an operating temperature of 280°C and relative humidity of 25% RH. We can see from the figure that the nine-response cycles are successively recorded, and the gas sensor based on $In_{10}Cd_1$ nanofibers show good sensitivities to formaldehyde. As shown in the inset in Figure 6 that the response and

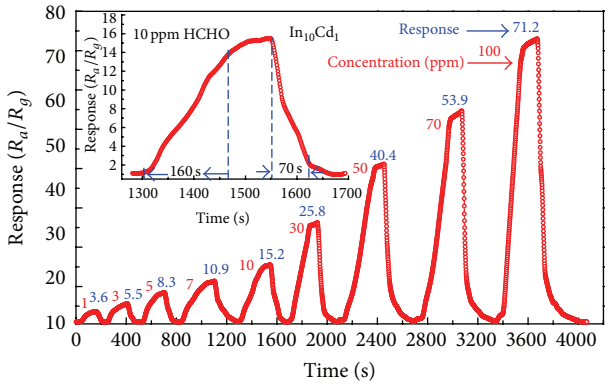

FIGURE 6: Response changes with time to different HCHO concentrations (1~100 ppm) for sensors based on $In_{10}Cd_1$ nanofibers at an operating temperature of 280°C; the inset is the response and recovery time curves to 10 ppm HCHO for sensor based on $In_{10}Cd_1$ nanofibers.

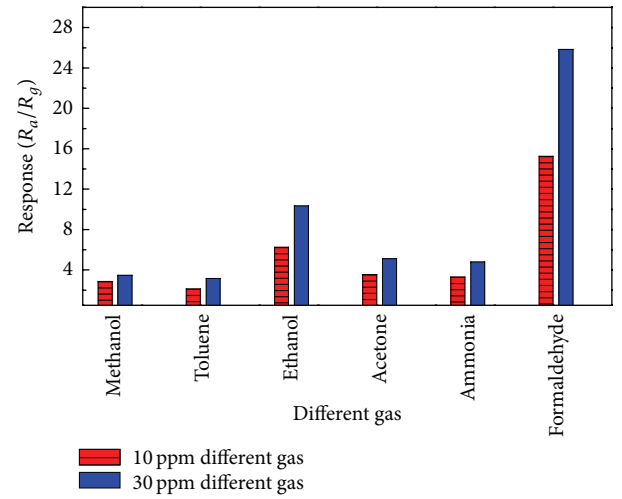

FIGURE 7: Responses of the sensor based on $In_{10}Cd_1$ nanofibers to 10 and 30 ppm different gases.

recovery times of the sensor based on $In_{10}Cd_1$ nanofibers were 160 s and 70 s to 10 ppm formaldehyde, respectively.

Figure 7 shows the responses of the sensor based on $In_{10}Cd_1$ nanofibers to formaldehyde, ethanol, methanol, toluene, acetone, and ammonia with concentration of 10 ppm and 30 ppm, respectively. The results indicated that the sensor based on $In_{10}Cd_1$ nanofibers exhibited a significantly higher response to formaldehyde than to other gases at the operating temperature of 280°C.

3.3. Mechanisms of HCHO-Sensing Based on Cd-Loaded In_2O_3 Nanofibers. In_2O_3 is an *n*-type semiconductor material and its gas sensing mechanism can be explained by the doping mechanism and external chemisorbed oxygen model. Change of material resistance is dependent on the species and the amount of oxygen chemisorbed on the surface of the sensing material. When metal ions Cd^{2+} was doped into In_2O_3 nanofibers, part of free electrons in In_2O_3 recombined with new generated holes as reaction (4), which is caused by that part of In^{3+} in In_2O_3, was displaced by Cd^{2+} as reaction (3) [30]. Meanwhile, when the *n*-type semiconductor oxides such as $In_{10}Cd_1$ are exposed in the air, the oxygen molecules will be adsorbed onto the surfaces of the materials and ionized to oxygen ions in the main form of O^- [31] by capturing free electrons from the conduction band of the oxide as shown in Figure 8(a) and reaction (5) [32]. The reaction (3)–(5) will cause a decrease of the carrier concentration and an increase of the resistance in air (R_a), which will enhance the response of the material ($S = R_a/R_g$) according to the following:

$$Cd_{In}^{x} \longleftrightarrow Cd_{In}^{\prime} h^{+} \longleftrightarrow Cd_{In}^{\prime} + h^{+} \quad (3)$$

$$h^{+} + e^{-} \longleftrightarrow \text{null} \quad (4)$$

$$O_{2\,(gas)} \longleftrightarrow O_{2\,(ads)} + e^{-} \longleftrightarrow O_{2\,(ads)}^{-} + e^{-} \longleftrightarrow O_{(ads)}^{-} \quad (5)$$

When the *n*-type semiconductor oxides ($In_{10}Cd_1$) meet reducing gas like formaldehyde, the formaldehyde gas molecules react with the adsorbed oxygen ions (O^-) generated by reaction (5) and release the trapped electrons back to the conduction band of the sensitive materials as shown in Figure 8(b) and reaction (6), resulting in an increase of the carrier concentration and a decrease of the resistance (R_g) [33]:

$$HCHO_{(g)} + O_{(ads)}^{-} \longrightarrow CHOOH_{(g)} + e^{-} \quad (6)$$

As we know that In_2O_3 nanofibers doped with certain concentration Cd may increase the selectivity and sensitivity and also reduce the response and recovery times of MOS gas sensors because the additive (Cd) changes the base oxides' interface state, which results in a variation of the surface barrier height and finally leads to a conductance change on the base oxide [34]. But Cd-loaded In_2O_3 nanofibers with other Cd/In molar ratios such as 1/20 and 1/1 did not enhance the formaldehyde gas properties as we expected. Next, the role of different concentration of Cd on improving the sensing properties will be discussed from two aspects: the surface-to-volume ratio of the sensing material and the resistance of the sensor (R_a). Grain sizes of Cd-loaded In_2O_3 nanofibers increased with the increasing of Cd/In molar ratios. As we know, the surface-to-volume ratio increases with the decrease of gain size [35], which will cause improvement of the surface reactivity. In other words, a decrease of the gain size will enhance sensor response. As we mentioned before, with Cd^{2+}doping, the resistance of the sensor in air (R_a) will increase. And with the increase of the Cd-doped concentration, there will be more Cd^{2+}replace In^{3+}, meaning R_a will become bigger. Since the response of sensors is defined as: $S = R_a/R_g$, so the increase of R_a means the increase of response. Moreover, when Cd/In molar ratio is 1/1, new phase $CdIn_2O_4$ forms, which may cause the decrease of Cd doping concentration. The effect of those two aspects on sensing response is opposite. When the Cd/In molar ratio is 1/10,

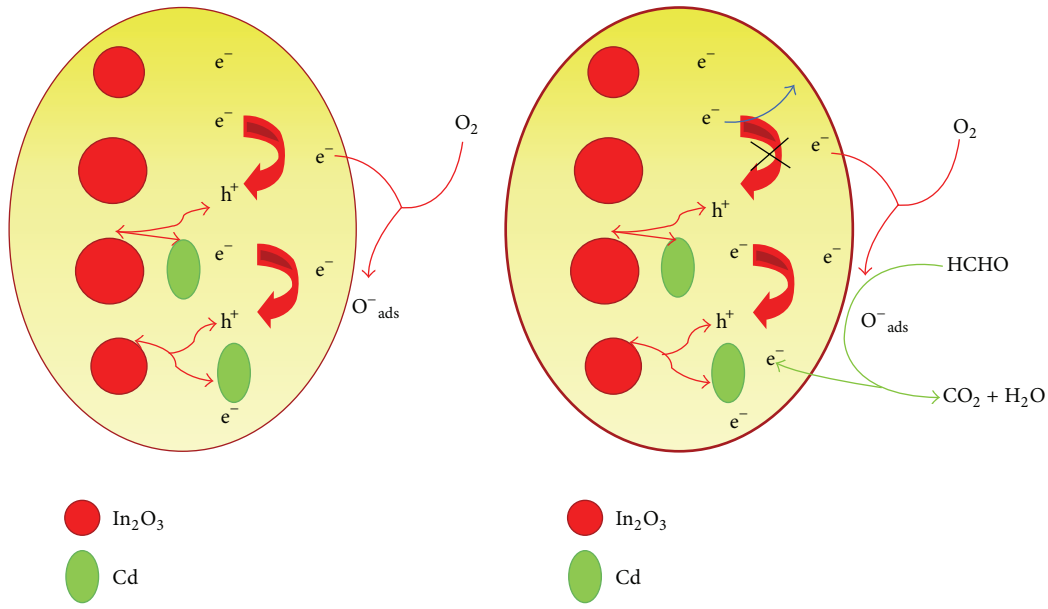

FIGURE 8: The adsorption model of Cd-loaded In_2O_3 nanofibers in air and in formaldehyde gases, respectively.

with the influence of those two aspects, the sensing response achieves the highest in this experiment.

4. Conclusion

In summary, Cd-loaded In_2O_3 nanofibers with different Cd/In molar ratios from 1/20 to 1/1 were prepared by an electrospinning method. The hollow and porous nanofibers are composed of nanoparticles. The average diameter and the nanoparticles size of Cd-loaded In_2O_3 nanofibers increase with increasing Cd/In molar ratio. Formaldehyde gas sensors were fabricated by coating the obtained materials onto a ceramic tube with a pair of gold electrodes and heaters. The sensors based on Cd-loaded In_2O_3 nanofibers with Cd/In molar ratio 1/10 ($In_{10}Cd_1$) exhibited higher response in formaldehyde concentration range of 0.5~100 ppm at operating temperature of 280°C than other materials with different Cd/In molar ratios. The response of $In_{10}Cd_1$ based sensors possesses good linearity with formaldehyde concentration in the range of 10~100 ppm. The response and recovery times of the sensor based on $In_{10}Cd_1$ nanofibers were 160 s and 70 s to 10 ppm formaldehyde, respectively. The sensor also exhibited a significantly higher response to formaldehyde than to ethanol, methanol, toluene, acetone, and ammonia. Cd-loaded In_2O_3 hollow and porous nanofibers with Cd/In molar ratio 1/10 ($In_{10}Cd_1$) have smaller grain size than In_1Cd_1 and larger resistance of the sensor in air than $In_{20}Cd_1$, which could be one reason for better sensitivity of $In_{10}Cd_1$ than other ratios materials.

Conflict of Interests

The authors declare that there is no conflict of interests regarding the publication of this paper.

Acknowledgments

The authors thank The National Natural Science Foundation of China (61176068, 61131004, and 61001054) and the 973 Projects (2011CB302105) for financial support.

References

[1] N. Noisel, M. Bouchard, and G. Carrier, "Evaluation of the health impact of lowering the formaldehyde occupational exposure limit for Quebec workers," *Regulatory Toxicology and Pharmacology*, vol. 48, no. 2, pp. 118–127, 2007.

[2] S. Huang, H. Qin, P. Song et al., "The formaldehyde sensitivity of $LaFe_{1-x}$ Zn_x O 3-based gas sensor," *Journal of Materials Science*, vol. 42, no. 24, pp. 9973–9977, 2007.

[3] N. H. Al-Hardan, M. J. Abdullah, A. Abdul Aziz, H. Ahmad, and L. Y. Low, "ZnO thin films for VOC sensing applications," *Vacuum*, vol. 85, no. 1, pp. 101–106, 2010.

[4] D. Richter, A. Fried, B. P. Wert, J. G. Walega, and F. K. Tittel, "Development of a tunable mid-IR difference frequency laser source for highly sensitive airborne trace gas detection," *Applied Physics B*, vol. 75, no. 2-3, pp. 281–288, 2002.

[5] R. L. Bunde, E. J. Jarvi, and J. J. Rosentreter, "A piezoelectric method for monitoring formaldehyde induced crosslink formation between poly-lysine and poly-deoxyguanosine," *Talanta*, vol. 51, no. 1, pp. 159–171, 2000.

[6] S. K. Gupta, A. Joshi, and K. Manmeet, "Development of gas sensors using ZnO nanostructures," *Journal of Chemical Sciences*, vol. 122, no. 1, pp. 57–62, 2010.

[7] X. Lou, C. Peng, X. Wang, and W. Chu, "Gas-sensing properties of nanostructured SnO_2-based sensor synthesized with different methods," *Vacuum*, vol. 81, no. 7, pp. 883–889, 2007.

[8] J.-A. Park, J. Moon, S.-J. Lee, S. H. Kim, T. Zyung, and H. Y. Chu, "Structure and CO gas sensing properties of electrospun TiO_2 nanofibers," *Materials Letters*, vol. 64, no. 3, pp. 255–257, 2010.

[9] Z. Li, Y. Fan, and J. Zhan, "In_2O_3 nanofibers and nanoribbons: preparation by electrospinning and their formaldehyde gas-sensing properties," *European Journal of Inorganic Chemistry*, no. 21, pp. 3348–3353, 2010.

[10] X. Lai, D. Wang, N. Han et al., "Ordered arrays of bead-chain-like In_2O_3 nanorods and their enhanced sensing performance for formaldehyde," *Chemistry of Materials*, vol. 22, no. 10, pp. 3033–3042, 2010.

[11] L. Guo, X. Shen, G. Zhu, and K. Chen, "Preparation and gas-sensing performance of In_2O_3 porous nanoplatelets," *Sensors and Actuators B*, vol. 155, no. 2, pp. 752–758, 2011.

[12] S. K. Lim, S.-H. Hwang, D. Chang, and S. Kim, "Preparation of mesoporous In_2O_3 nanofibers by electrospinning and their application as a CO gas sensor," *Sensors and Actuators B*, vol. 149, no. 1, pp. 28–33, 2010.

[13] A. Kolmakov and M. Moskovits, "Chemical sensing and catalysis by one-dimensional metal-oxide nanostructures," *Annual Review of Materials Research*, vol. 34, pp. 151–180, 2004.

[14] C. Soldano, E. Comini, C. Baratto, M. Ferroni, G. Faglia, and G. Sberveglieri, "Metal oxides mono-dimensional nanostructures for gas sensing and light emission," *Journal of the American Ceramic Society*, vol. 95, no. 3, pp. 831–850, 2012.

[15] B. Wang, Y. Zhao, L. Hu et al., "Improved and excellent CO sensing properties of Cu-doped TiO_2 nanofibers," *Chinese Science Bulletin*, vol. 55, no. 3, pp. 228–232, 2010.

[16] M. T. Hunley and T. E. Long, "Electrospinning functional nanoscale fibers: a perspective for the future," *Polymer International*, vol. 57, no. 3, pp. 385–389, 2008.

[17] W. Zheng, X. Lu, W. Wang et al., "A highly sensitive and fast-responding sensor based on electrospun In_2O_3 nanofibers," *Sensors and Actuators B*, vol. 142, no. 1, pp. 61–65, 2009.

[18] X. Wang, J. Zhang, Z. Zhu, and J. Zhu, "Effect of Pd^{2+} doping on ZnO nanotetrapods ammonia sensor," *Colloids and Surfaces A*, vol. 276, no. 1–3, pp. 59–64, 2006.

[19] N. S. Ramgir, Y. K. Hwang, S. H. Jhung et al., "CO sensor derived from mesostructured Au-doped SnO_2 thin film," *Applied Surface Science*, vol. 252, no. 12, pp. 4298–4305, 2006.

[20] V. B. Gaikwad, M. K. Deore, P. K. Khanna et al., "Studies on gas sensing performance of pure and nano-Ag doped ZnO thick film resistors," *Recent Advances in Sensing Technology*, vol. 49, pp. 293–307, 2009.

[21] J. Wang, B. Zou, S. Ruan, J. Zhao, Q. Chen, and F. Wu, "HCHO sensing properties of Ag-doped In_2O_3 nanofibers synthesized by electrospinning," *Materials Letters*, vol. 63, no. 20, pp. 1750–1753, 2009.

[22] V. D. Kapse, S. A. Ghosh, G. N. Chaudhari, F. C. Raghuwanshi, and D. D. Gulwade, "H_2S sensing properties of La-doped nanocrystalline In_2O_3," *Vacuum*, vol. 83, no. 2, pp. 346–352, 2008.

[23] S. T. Shishiyanu, T. S. Shishiyanu, and O. I. Lupan, "Sensing characteristics of tin-doped ZnO thin films as NO_2 gas sensor," *Sensors and Actuators B*, vol. 107, no. 1, pp. 379–386, 2005.

[24] T. Chen, Z. Zhou, and Y. Wang, "Effects of calcining temperature on the phase structure and the formaldehyde gas sensing properties of CdO-mixed In_2O_3," *Sensors and Actuators B*, vol. 135, no. 1, pp. 219–223, 2008.

[25] A. Cabot, J. Arbiol, J. R. Morante, U. Weimar, N. Bârsan, and W. Göpel, "Analysis of the noble metal catalytic additives introduced by impregnation of as obtained SnO_2 sol-gel nanocrystals for gas sensors," *Sensors and Actuators B*, vol. 70, no. 1–3, pp. 87–100, 2000.

[26] X. Xu, H. Fan, Y. Liu, L. Wang, and T. Zhang, "Au-loaded In_2O_3 nanofibers-based ethanol micro gas sensor with low power consumption," *Sensors and Actuators B*, vol. 160, no. 1, pp. 713–719, 2011.

[27] L. Xu, B. Dong, Y. Wang et al., "Porous In_2O_3:RE (RE = Gd, Tb, Dy, Ho, Er, Tm, Yb) nanotubes: electrospinning preparation and room gas-sensing properties," *Journal of Physical Chemistry C*, vol. 114, no. 19, pp. 9089–9095, 2010.

[28] P. J. Yao, J. Wang, W. L. Chu, and Y. W. Hao, "Preparation and characterization of $La_{1-x}SrxFeO_3$ materials and their formaldehyde gas-sensing properties," *Journal of Materials Science*, vol. 48, no. 1, pp. 441–450, 2013.

[29] V. E. Henrich, "The surfaces of metal oxides," *Reports on Progress in Physics*, vol. 48, no. 11, pp. 1481–1541, 1985.

[30] J. Lao, J. Huang, D. Wang, and Z. Ren, "Self-assembled In_2O_3 nanocrystal chains and nanowire networks," *Advanced Materials*, vol. 16, no. 1, pp. 65–69, 2004.

[31] N. Yamazoe, J. Fuchigami, M. Kishikawa, and T. Seiyama, "Interactions of tin oxide surface with O_2, H_2O and H_2," *Surface Science*, vol. 86, pp. 335–344, 1979.

[32] K. D. Schierbaum, U. Weimar, W. Göpel, and R. Kowalkowski, "Conductance, work function and catalytic activity of SnO_2-based gas sensors," *Sensors and Actuators B*, vol. 3, no. 3, pp. 205–214, 1991.

[33] I. Castro-Hurtado, J. Herrán, G. Mandayo, and E. Castaño, "SnO_2-nanowires grown by catalytic oxidation of tin sputtered thin films for formaldehyde detection," *Thin Solid Films*, vol. 520, no. 14, pp. 4792–4796, 2012.

[34] P. P. Chen, J. Wang, and P. J. Yao, "Synthesis and gas sensitivity of In_2O_3/CdO composite," *Acta Physico-Chimica Sinica*, vol. 28, no. 6, pp. 1539–1544, 2012.

[35] G. Korotcenkov, V. Brinzari, V. Golovanov, and Y. Blinov, "Kinetics of gas response to reducing gases of SnO_2 films, deposited by spray pyrolysis," *Sensors and Actuators B*, vol. 98, no. 1, pp. 41–45, 2004.